Evolution of black carbon heterogeneity and optical absorption during atmospheric aging

Qiqi Mo[1], Jie Sun[1], Tong Liu[1], Gang Zhao[1*], Fengjun Shen, Xinlei Lv[1], Ziye Zhang[1], Yunxiao Li[1], Batu Alaxi[1], Weili Lin[1]

[1]Key Laboratory of Ecology and Environment in Minority Areas, Minzu University of China, National Ethnic Affairs Commission, Beijing 100081, China

Correspondence to: Gang Zhao (gangz@muc.edu.cn)

Table S1 to Table S3
Figure S1 to Figure S9

Table S1. Environmental and temporal input parameters prescribed in the baseline simulation.

Model input	Prescribed value
Relative humidity	0.720 (72 %)
Latitude	32°3′ N
Longitude	120° E
Altitude	9 m
Start time	57,600 s (16:00 UTC)
Start day	146 (26 May)

Table S2. Gas-phase emission fluxes prescribed in the simulations.

Emitted gas species	Rate (mol m^{-2} s^{-1})
Sulfur dioxide	1.06×10^{-9}
Nitrogen dioxide	7.56×10^{-10}
Nitric oxide	1.44×10^{-10}
Ammonia	8.93×10^{-9}
Carbon monoxide	1.96×10^{-9}
Acetaldehyde	4.25×10^{-12}
Ethene	4.62×10^{-11}
Isoprene	6.03×10^{-12}

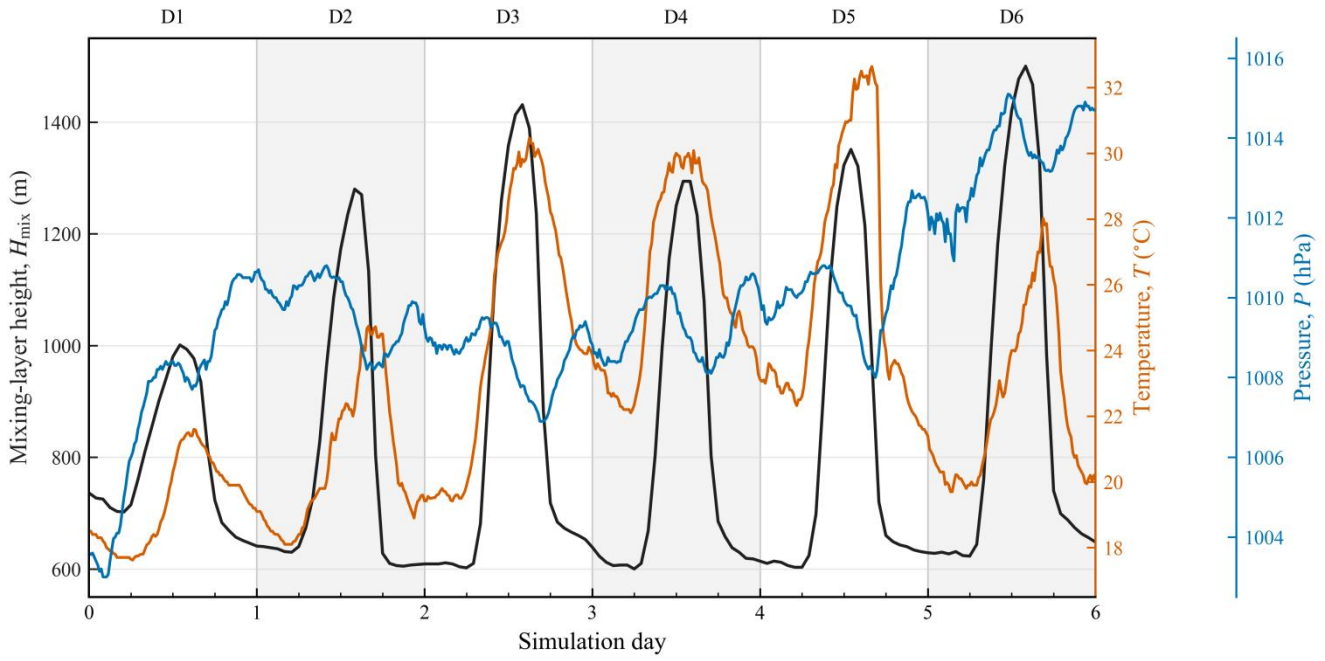

Figure S1: Six-day time series of the mixing-layer height, temperature, and pressure prescribed in the PartMC–MOSAIC simulations.

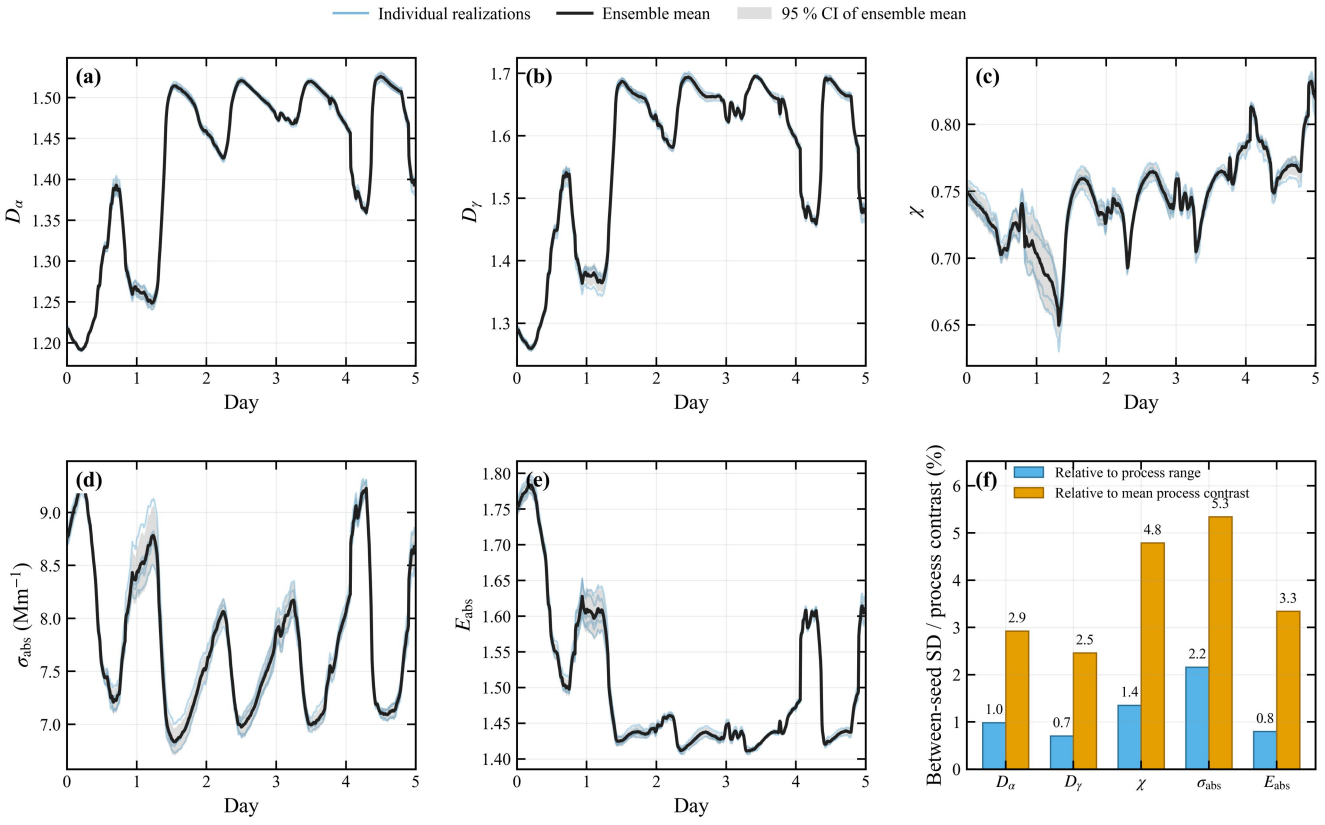

Figure S2: Monte Carlo ensemble uncertainty in BC mixing-state and optical metrics from five independent all-process simulations.

Table S3. Prescribed densities of individual aerosol components used in the particle-volume calculations.

Aerosol species	Density (kg m^{-3})
SO_4	1800
NO_3	1800
Cl	2200
NH_4	1800
MSA	1800
ARO1	1400
ARO2	1400
ALK1	1400
OLE1	1400
API1	1400
API2	1400
LIM1	1400
LIM2	1400
CO_3	2600
Na	2200
Ca	2600
OIN	2600
OC	1000
BC	1800
H_2O	1000

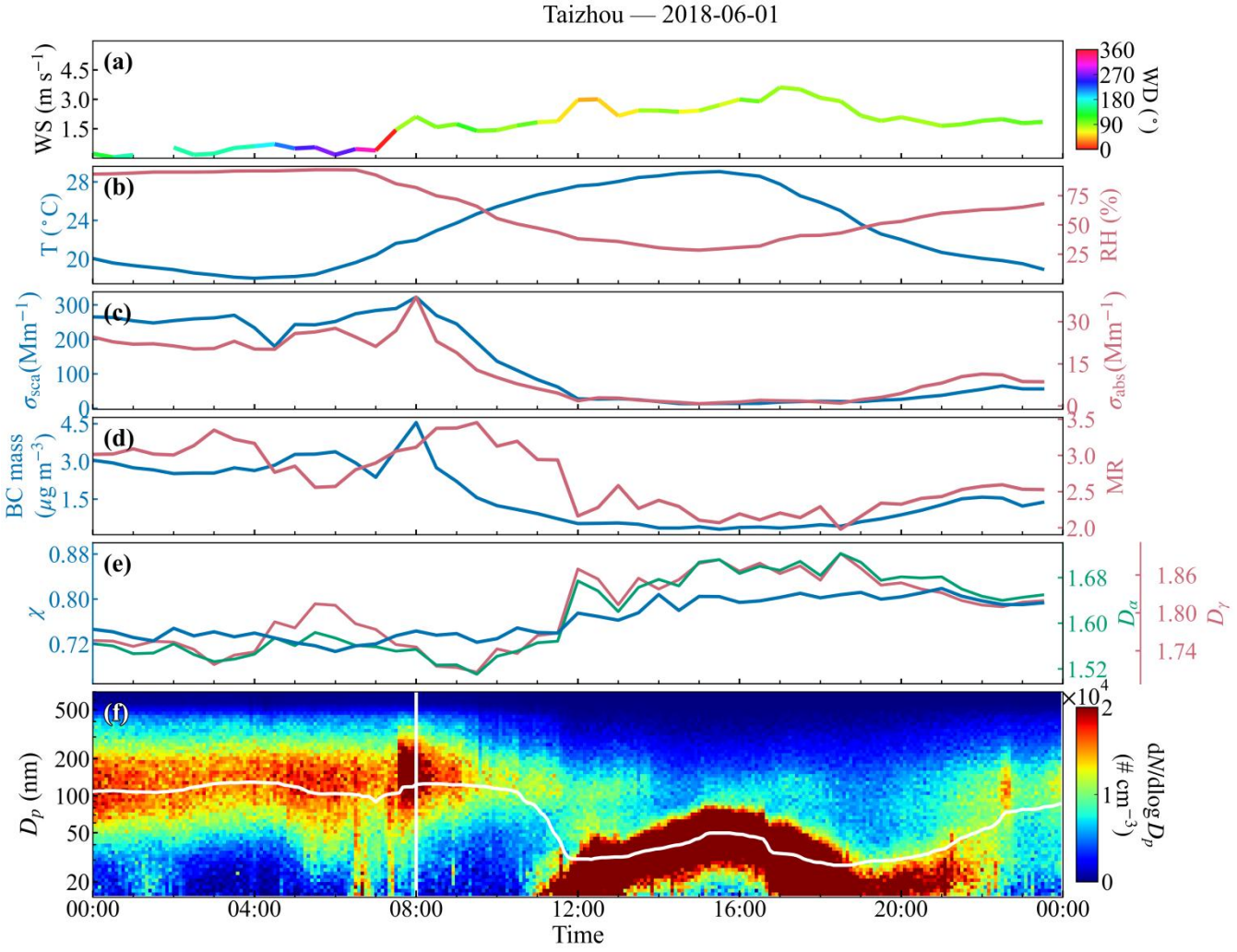

Figure S3: Time series of (a) wind speed (WS) and wind direction (WD); (b) temperature (T) and relative humidity (RH); (c) the aerosol scattering coefficient σ_{sca} and BC absorption coefficient (σ_{abs}); (d) BC mass concentration and the non-BC-to-BC mass ratio (MR); (e) the BC mixing-state index (χ), average particle diversity (D_α), and bulk population diversity (D_γ); and (f) the particle number size distribution (PNSD) as a function of particle diameter (D_p) in Taizhou on 1 June 2018. The white curve in (f) represents the smoothed median (D_p), and the colour scale denotes ($\mathrm{d}N/\mathrm{d}\log D_p$).

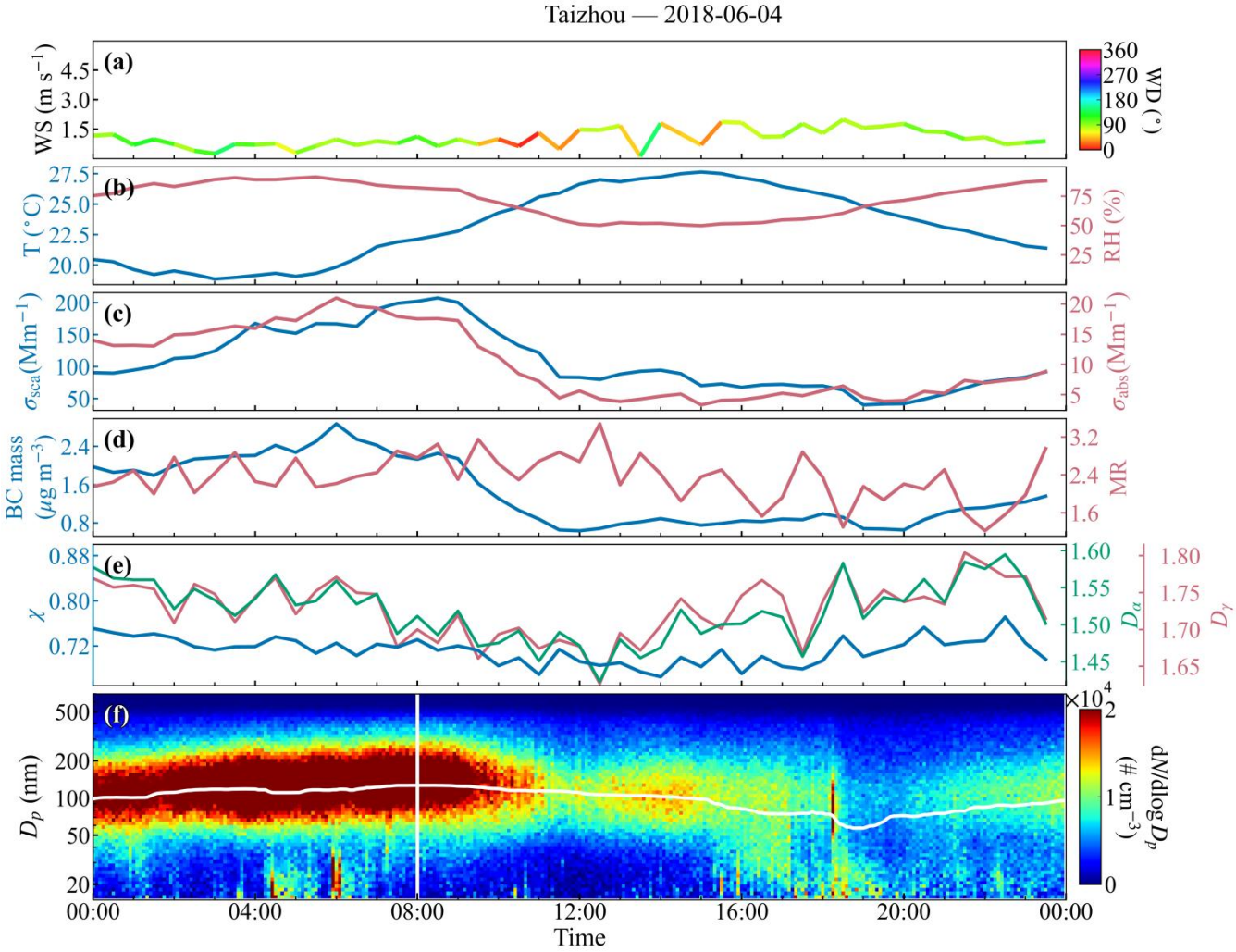

Figure S4: Time series of (a) WS and WD; (b) T and RH; (c) σ_{sca} and σ_{abs}; (d) MR; (e) χ, D_α, and D_γ; and (f) PNSD as a function of D_p in Taizhou on 4 June 2018. The white curve in (f) represents the smoothed median (D_p), and the colour scale denotes ($\mathrm{d}N/\mathrm{d}\log D_p$).

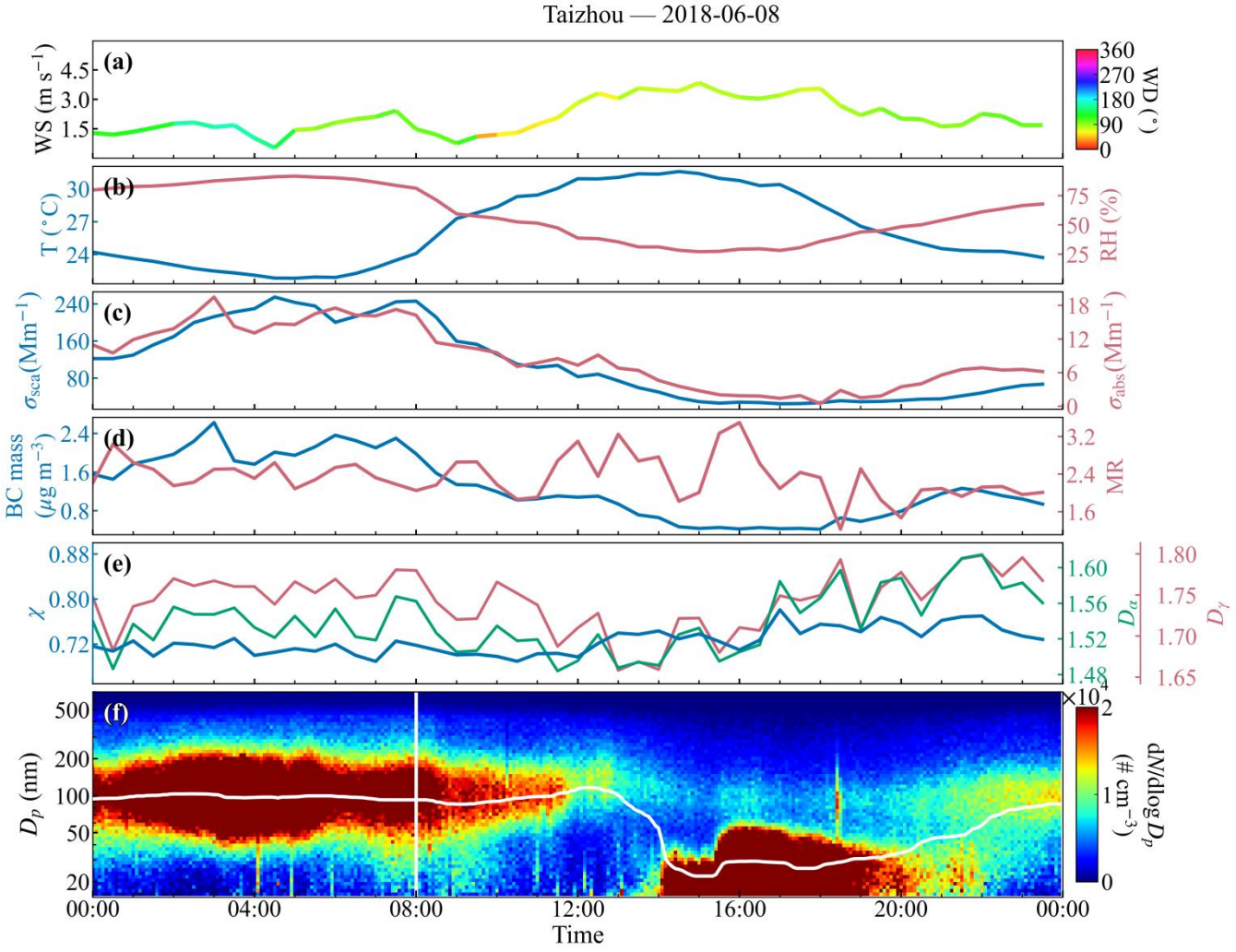

Figure S5: Time series of (a) WS and WD; (b) T and RH; (c) σ_{sca} and σ_{abs}; (d) MR; (e) χ, D_α, and D_γ; and (f) PNSD as a function of D_p in Taizhou on 8 June 2018. The white curve in (f) represents the smoothed median (D_p), and the colour scale denotes ($\mathrm{d}N/\mathrm{d}\log D_p$).

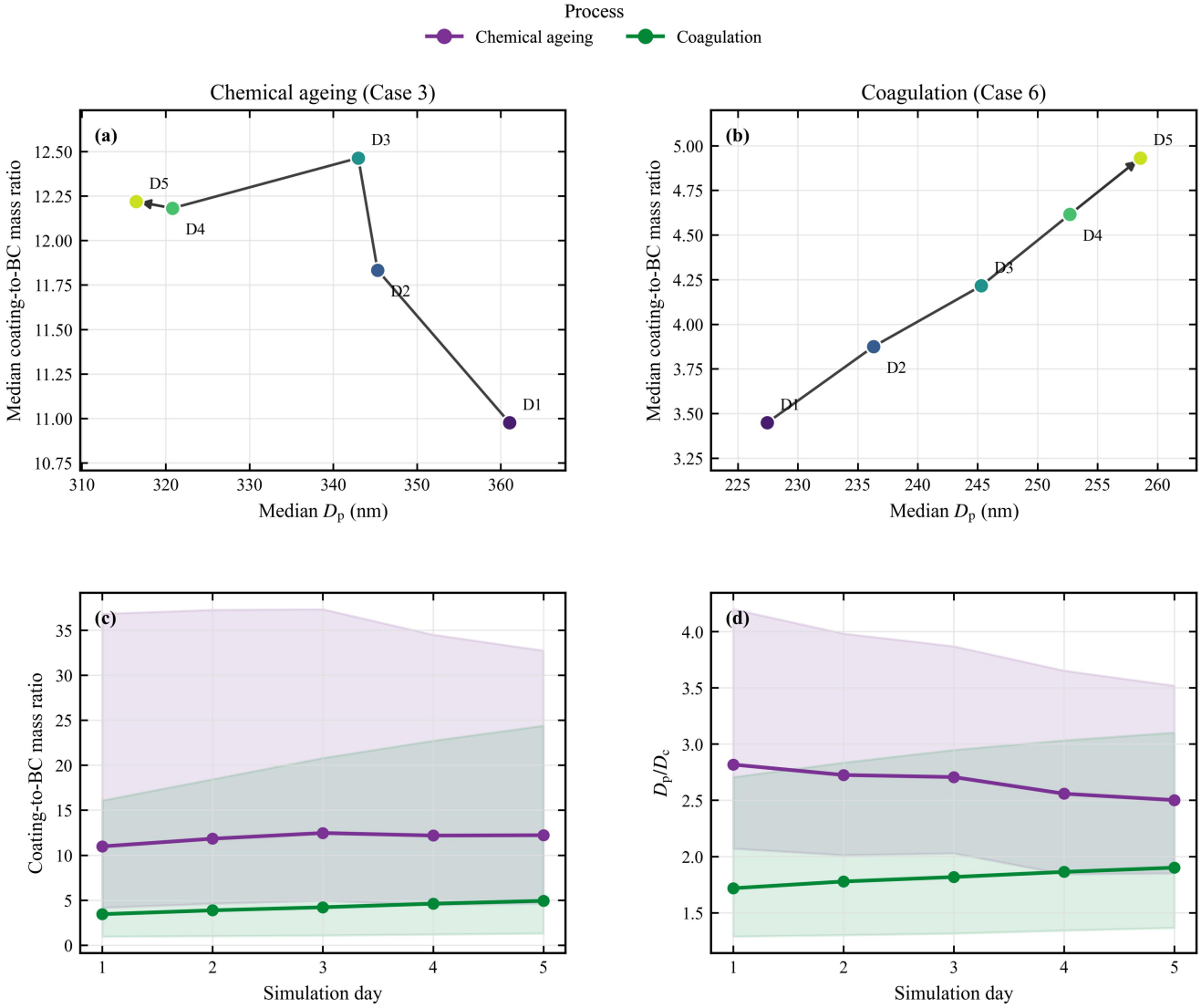

Figure S6: Contrasting daily evolution of BC particle size and coating properties under chemical ageing and coagulation. Panels (a) and (b) show the D1−D5 trajectories of median D_p and coating-to-BC mass ratio, with independently scaled axes. Panels (c) and (d) show the daily medians and P10−P90 ranges of the coating-to-BC mass ratio and D_p/D_c, respectively.

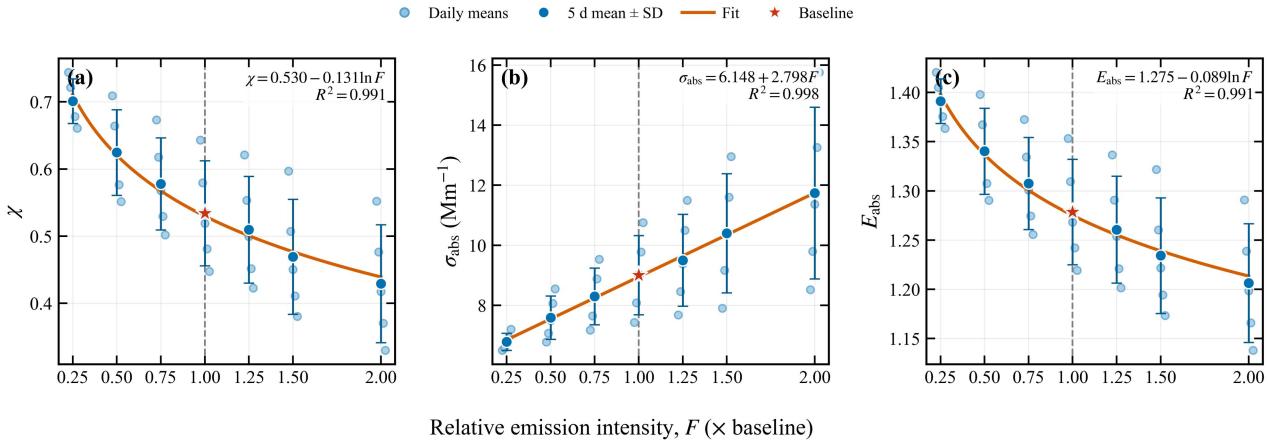

Figure S7: Sensitivity of the BC mixing-state index and absorption properties to fresh-particle emission intensity in the emission-only PartMC–MOSAIC simulations. Responses of (a) the mixing-state index (χ), (b) the BC absorption coefficient (σ_{abs}) at 880 nm, and (c) the population-integrated absorption enhancement factor (E_{abs}) to the relative emission intensity F, ranging from 0.25 to 2.00 times the baseline value. The baseline emission scaling rate was 0.009 and is indicated by the grey dashed line and red star. Pale-blue symbols represent daily means after excluding the first 24 h initialization period, while dark-blue symbols and error bars denote the corresponding 5 d means and standard deviations among daily means. Orange curves show the fitted relationships based on the seven emission-intensity simulations.

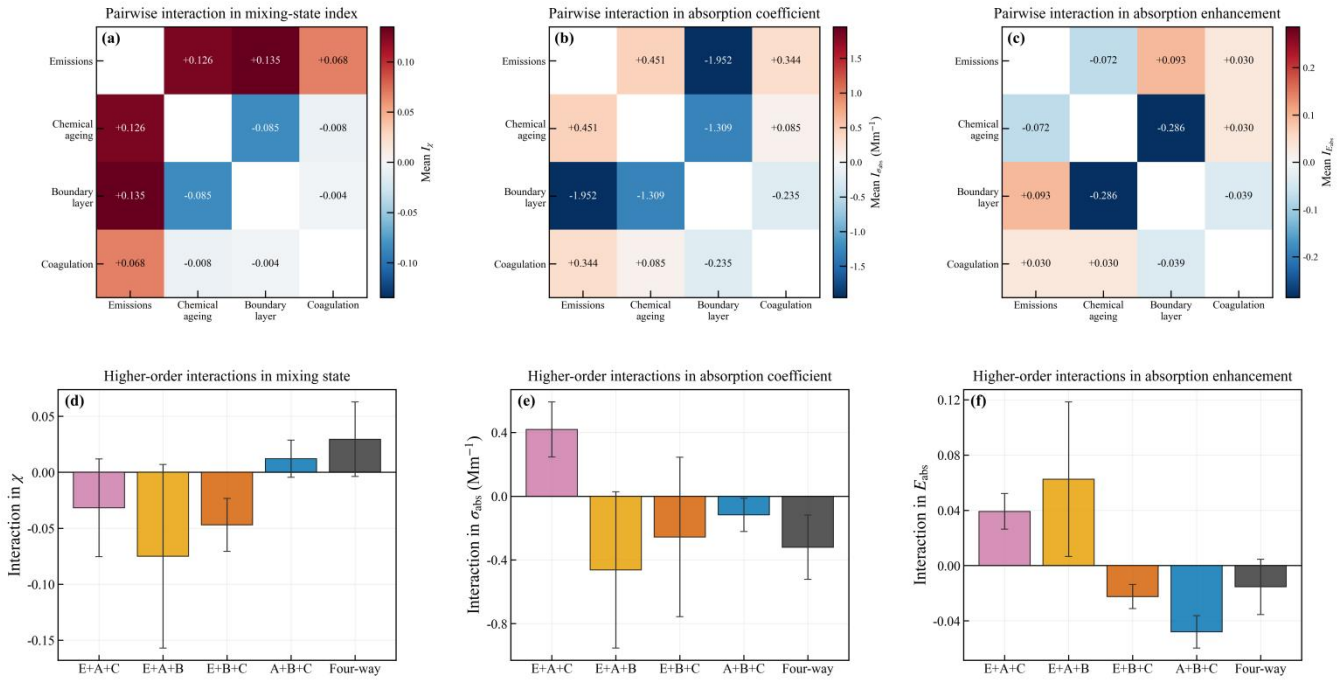

Figure S8: Interactions among emissions (E), chemical ageing (A), boundary-layer variation (B), and coagulation (C) in simulated χ, σabs, and Eabs. (a–c) Mean pairwise interactions; (d–f) higher-order interactions. Positive and negative values indicate responses above and below the additive expectation, respectively. Error bars denote temporal standard deviations over the five analysed days.

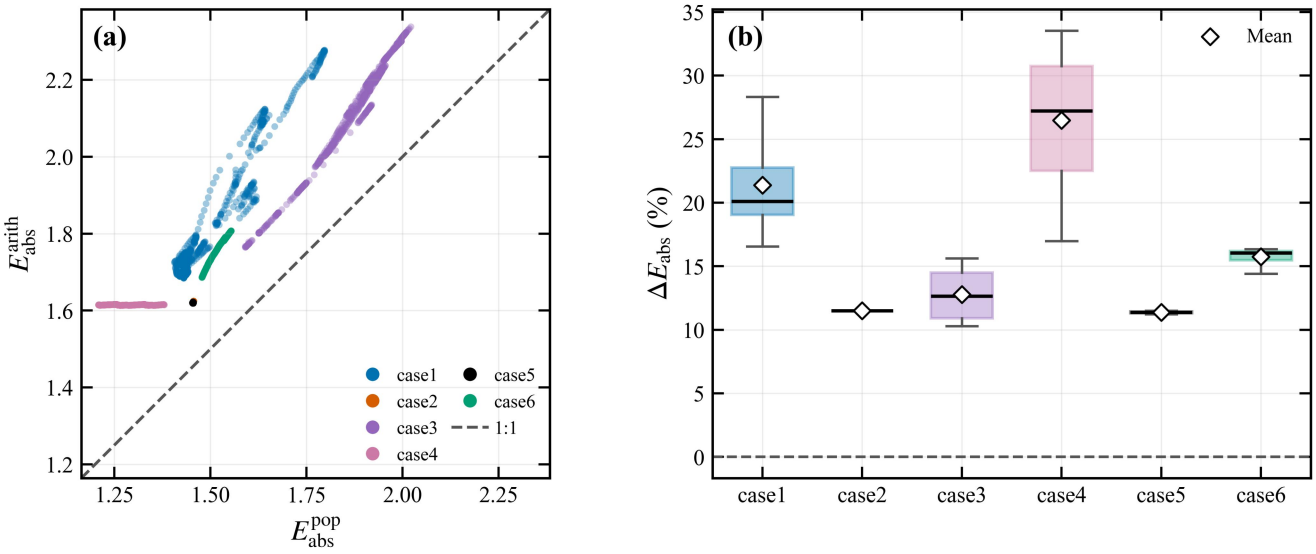

Figure S9: Comparison of population-integrated (E_{abs}^{pop}) and particle arithmetic-mean (E_{abs}^{arith}) absorption enhancement at 880 nm. (a) Time-resolved comparison, with the dashed line denoting 1:1 agreement. (b) Relative difference, ($\Delta E_{abs}=(E_{abs}^{arith}-E_{abs}^{pop})/E_{abs}^{pop}\times 100\ \%$). Diamonds indicate means.